Can ^{111}In-RGD$_2$ Monitor Response to Therapy in Head and Neck Tumor Xenografts?

Samantha Y.A. Terry[1,2], Keelara Abiraj[3], Jasper Lok[4], Danny Gerrits[1], Gerben M. Franssen[1], Wim J.G. Oyen[1], and Otto C. Boerman[1]

[1]Department of Radiology and Nuclear Medicine, Radboud University Medical Center, Nijmegen, The Netherlands; [2]Department of Imaging Sciences, Kings College London, London, United Kingdom; [3]Roche Pharmaceutical Research and Early Development (pRED), Roche Innovation Center Basel, Basel, Switzerland; and [4]Department of Radiation Oncology, Radboud University Medical Center, Nijmegen, The Netherlands

RGD (arginylglycylaspartic acid)–based imaging tracers allow specific imaging of integrin $\alpha_v\beta_3$ expression, proteins overexpressed during angiogenesis; however, few studies have investigated the potential of these tracers to monitor responses of antiangiogenic or radiation therapy. In the studies presented here, ^{111}In-RGD$_2$ was assessed for its potential as an imaging tool to monitor such responses to therapies. **Methods:** DOTA-E-[c(RGDfK)]$_2$ was radiolabeled with ^{111}In (^{111}In-RGD$_2$), and biodistribution studies were performed in mice with subcutaneous FaDu or SK-RC-52 xenografts after treatment with either antiangiogenic therapy (bevacizumab or sorafenib) or tumor irradiation (10 Gy). Micro-SPECT imaging studies and subsequent quantitative analysis were also performed. The effect of bevacizumab, sorafenib, or radiation therapy on tumor growth was determined. **Results:** The uptake of ^{111}In-RGD$_2$ in tumors, as determined from biodistribution studies, correlated well with that quantified from micro-SPECT images, and both showed that 15 d after irradiation ^{111}In-RGD$_2$ uptake was enhanced. Specific or nonspecific uptake of ^{111}In-RGD$_2$ in FaDu or SK-RC-52 xenografts was not affected after antiangiogenic therapy, except in head and neck squamous cell carcinoma 19 d after the start of sorafenib therapy ($P < 0.05$). The uptake of ^{111}In-RGD$_2$ followed tumor volume in studies featuring antiangiogenic therapy. However, the uptake of ^{111}In-RGD$_2$ in FaDu xenografts was decreased as early as 4 h after tumor irradiation, despite nonspecific uptake remaining unaltered. Tumor growth was inhibited after antiangiogenic or radiation therapy. **Conclusion:** Here, it is suggested that ^{111}In-RGD$_2$ could allow in vivo monitoring of angiogenic responses after radiotherapy and may therefore prove a good clinical tool to monitor angiogenic responses early after the start of radiotherapy in patients with head and neck squamous cell carcinoma. Despite clear antitumor efficacy, antiangiogenic therapy did not alter tumor uptake of ^{111}In-RGD$_2$, indicating that integrin expression was not altered.

Key Words: integrin $\alpha_v\beta_3$; dimeric RGD; monitor response; antiangiogenic therapy; radiotherapy

J Nucl Med 2014; 55:1849–1855
DOI: 10.2967/jnumed.114.144394

Radiolabeled RGD (arginylglycylaspartic acid) peptides allow specific and noninvasive in vivo imaging of integrin $\alpha_v\beta_3$ expression, a receptor overexpressed in the early stages of angiogenesis (*1*). Angiogenesis describes the formation of new blood vessels from preexisting vessels and is often regarded as one of the hallmarks of cancer (*2*). The literature encompasses a plethora of papers about the imaging of integrin $\alpha_v\beta_3$ by both PET and SPECT (*3–5*). The validation of RGD-based imaging probes often included in vivo tumor xenograft models in which integrin $\alpha_v\beta_3$ was constitutively overexpressed on tumor cells (*6–13*). More recently, radiolabeled DOTA-E-[c(RGDfK)]$_2$ was also shown to allow imaging of angiogenesis itself, when used in a tumor model in which integrin $\alpha_v\beta_3$ was expressed solely on the tumor vasculature (*14*).

Despite the variety of previously synthesized RGD-based tracers (*5*) and constant production of newly synthesized, slightly superior, tracers, only a handful of studies have been performed to determine their applicability to the clinic. The first study to suggest that monomeric RGD tracers, namely ^{18}F-galacto-RGD, could monitor the therapeutic efficacy of anticancer therapy targeting integrin $\alpha_v\beta_3$ was performed in mice bearing M21 human melanoma xenografts (*15*). More recently, it was also found that monomeric RGD tracers can monitor response to treatment with either antiangiogenic or antimigratory and antiproliferative therapy (*16–18*). So far, only one publication suggests that dimeric RGD peptide tracers can monitor response to therapy, here the antiangiogenic linifanib (*19*).

Increased applications of antiangiogenic therapies, such as the anti–vascular endothelial growth factor antibody bevacizumab (Avastin; Roche Pharma), and small-molecule tyrosine kinase inhibitors, such as sorafenib (*20*), have triggered an interest in specifically imaging angiogenesis using nuclear tracers. Monitoring response to antiangiogenic therapy with radiolabeled tracers, including but not limited to radiolabeled bevacizumab, has had its limitations (*5*). The focus of imaging angiogenic responses has recently moved toward using radiolabeled RGD peptides to provide specific and early feedback on the effect of antiangiogenic therapy on angiogenesis. These peptides are small with fast clearance from the blood, early imaging possibilities, and few issues regarding perfusion and permeability. If RGD-based tracers prove capable of monitoring angiogenic responses to therapy, they have the potential to select patients who might benefit from treatment with antiangiogenic drugs, beyond short-term tumor control. It is especially important to be able to monitor the efficacy of

Received Jun. 13, 2014; revision accepted Sep. 8, 2014.
For correspondence or reprints contact: Samantha Terry, Kings College London, Department of Imaging Sciences the Rayne Institute, 4th Floor, Lambeth Wing St. Thomas' Hospital, Westminster Bridge Rd., London, SE1 7EH United Kingdom.
E-mail: samantha.terry@kcl.ac.uk
Published online Oct. 27, 2014.

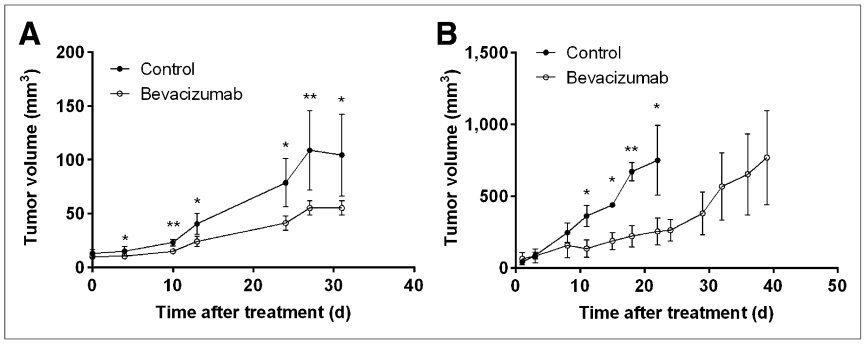

FIGURE 1. Tumor growth study of mice with SK-RC-52 (A) or FaDu (B) xenografts treated with bevacizumab. $^*P \leq 0.05$. $^{**}P \leq 0.01$.

antiangiogenic therapies early on, considering overall survival is prolonged in only a limited group of patients, yet most patients still encounter side effects such as hand–foot syndrome.

Imaging angiogenesis is also important when considering treatment resistance in head and neck squamous cell carcinoma (HNSCC) patients. There are several ways in which tumors become resistant to treatment, including enhanced angiogenesis in hypoxic tumor areas (*21*). Being able to noninvasively monitor early on whether patients respond to therapy would allow clinicians to determine whether the treatment should be adjusted.

Here, we use HNSCC xenograft models to determine whether ^{111}In-RGD$_2$ can monitor responses to antiangiogenic or radiation therapy early on. The novelty is the use of tumor models in which integrin $\alpha_v\beta_3$ is expressed only on angiogenic blood vessels (*14*). We also investigated the use of ^{111}In-RGD$_2$ as a tool to monitor antiangiogenic therapy in integrin $\alpha_v\beta_3$–positive tumors (*22*).

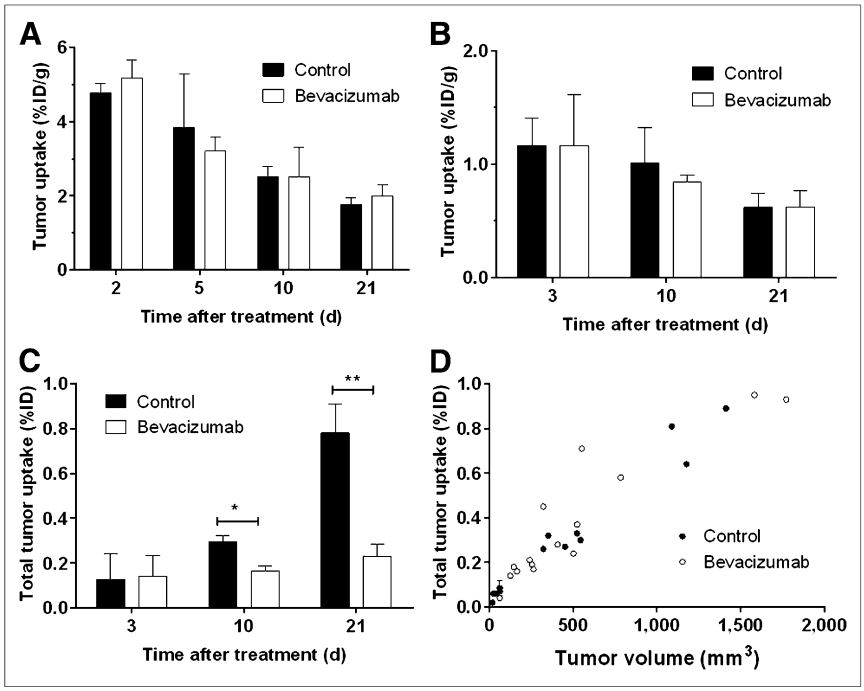

FIGURE 2. Bevacizumab therapy. Uptake of ^{111}In-RGD$_2$ in SK-RC-52 (A) or FaDu (B–D) tumor xenografts in mice treated with bevacizumab. (D) Tumor uptake of ^{111}In-RGD$_2$ in individual tumors plotted against tumor volume. $^*P \leq 0.05$. $^{**}P \leq 0.01$.

MATERIALS AND METHODS

Cell Culture and In Vivo Studies

FaDu human pharynx squamous cell carcinoma cells, lacking constitutive integrin $\alpha_v\beta_3$ expression, and SK-RC-52 human renal carcinoma cells, constitutively expressing integrin $\alpha_v\beta_3$, were cultured in RPMI 1640 medium with 10% (v/v) fetal calf serum and 1% glutamine (Invitrogen). Cells were maintained at 37°C in a humidified 5% CO_2 atmosphere and routinely passaged using a 0.25% trypsin/ethylenediaminetetraacetic acid solution (Invitrogen).

In vivo, tumor volumes were measured by caliper. All animal experiments were approved by the local Animal Welfare Committee in accordance with Dutch legislation and performed in accordance to their guidelines. A visual representation of the treatment schedule is presented in Supplemental Figure 1 (supplemental materials are available at http://jnm.snmjournals.org).

Antiangiogenic and Radiation Therapies

FaDu (5×10^6) or SK-RC-52 (2×10^6) cells in RPMI 1640 were injected subcutaneously on the right flank of female BALB/c *nu/nu* mice (Janvier). When tumors reached 100 or 10 mm^3, for FaDu and SK-RC-52 xenografts, respectively, mice were injected intraperitoneally with bevacizumab at 1 or 10 mg/kg in 200 μL of saline or vehicle alone (day 0). Bevacizumab or vehicle was administered on days 0, 4, and 8. In a separate study, mice bearing FaDu xenografts of 100 mm^3 were injected daily with sorafenib (0.25–1 mg/mouse) in 4% Cremophor and 3% ethanol in sterile saline or vehicle alone (intraperitoneally).

In irradiation studies, FaDu cells (1×10^6) in RPMI 1640 were injected subcutaneously in the right hind limb of female BALB/c *nu/nu* mice. When tumors reached 200 mm^3, anesthetized mice (isoflurane/air/O_2, 5% induction, 3% maintenance) were covered in custom-made lead shielding, to locally irradiate the tumor only, at 10 Gy using a 320 kV X-RAD system (RPS Services Limited) at 3.8 Gy per minute. Control mice were sham-irradiated. A visual representation of the treatment schedule in presented in Supplemental Figure 1.

Radiolabeling

One microgram of DOTA-E-[c(RGDfK)]$_2$ (Peptides International (*7*)) (E = glutamate, c = cyclic, RGD = arginylglycylaspartic acid, DOTA-E-[c(RGDfK)]$_2$ = RGD$_2$) in 0.1 M 2-(*N*-morpholino)ethanesulfonic acid, pH 5.5, was incubated with 0.5–20 MBq of $^{111}InCl_3$ (Malinckrodt Medical) for 20 min at 95°C. Purification and quality control were also performed as described previously to ensure that a radiochemical purity of 95% was achieved (*14*).

Biodistribution and Micro-SPECT/CT Imaging Studies

In biodistribution studies, mice with FaDu or SK-RC-52 xenografts, treated with or without antiangiogenic or radiation therapy, were injected intravenously with 1 μg of ^{111}In-RGD$_2$ (≤1MBq) in 200 μL of 0.5%

TABLE 1
Uptake (%ID/g) of ^{111}In-RGD$_2$ Plus 50 μg of RGD$_2$ in Mice Treated with Bevacizumab

	Tumor type			
	SK-RC-52		FaDu	
Time after treatment (d)	Control	Bevacizumab	Control	Bevacizumab
≤3	0.98 ± 0.02	0.89 ± 0.06	0.24 ± 0.04	0.26 ± 0.07
10	0.48 ± 0.05	0.48 ± 0.07	0.13 ± 0.02	0.18 ± 0.06
21	0.36 ± 0.02	0.31 ± 0.03	0.20 ± 0.05	0.17 ± 0.01

bovine serum albumin in phosphate-buffered saline. Mice were euthanized by CO_2/O_2 1 h after tracer injection. Blood, tumor, organs, and tissues were dissected, weighed, and counted in a γ counter, and the percentage injected dose per gram (%ID/g) within them determined. Non–receptor-mediated localization of the radiolabeled peptide was investigated by determining the biodistribution of ^{111}In-RGD$_2$ in the presence of an excess (50 μg) of unlabeled peptide.

In micro-SPECT imaging studies, mice with FaDu tumor xenografts were injected intravenously with 1 μg of ^{111}In-RGD$_2$ (20 MBq) after local irradiation. One hour after tracer injection, mice were scanned under anesthesia (isoflurane/air/O_2, 5% induction, 3% maintenance) using the U-SPECT-II/CT scanner (MILabs) (*23*). SPECT scans were acquired as 3 frames of 15 min, followed by a CT scan for anatomic reference (SPECT: spatial resolution 160 μm, 65 kV, 615 μA). SPECT scans, all frames combined, were reconstructed with software from MILabs, using an ordered-subset expectation maximization algorithm, with a voxel size of 0.4 mm.

Quantitative SPECT Analysis

Reconstructed micro-SPECT scans were coregistered with CT images using Inveon Research Workplace software (version 3.0; Siemens Preclinical Solutions). The regions of interest were determined using CT scans, and the mean voxel intensity within these was determined from SPECT scans. Mean voxel intensity values were converted to %ID/g using decay correction and a standard curve (mean voxel intensity vs. kBq) acquired by scanning and reconstructing known ^{111}In activities from 3.7 to 370 kBq in 200 μL in a 0.5-mL Eppendorf tube (Eppendorf) under the same conditions as the animal scans.

Immunohistochemistry

Flash-frozen tumor sections (5 μm) also used for the tumor uptake studies were stained for murine integrin β_3 (CD61), a marker of angiogenic integrin $\alpha_v\beta_3$, and 9F1, a marker of murine blood vessels, as described previously (*14*). In general, staining intensities for CD61 was weak, as target density was low, and strong, respectively. Slides were scored on the basis of the area of the section positively stained, with +, ++, and +++ equaling ≤5%, 6%–10%, and 11%–20%, respectively.

Statistical Analysis

Statistical analysis was performed using a 1-sample *t* test with GraphPad Prism (version 5.03; GraphPad Software). Statistical significance was represented as $P \leq 0.05$, 0.01, and 0.001. Data in tables, biodistribution, and quantitative SPECT studies are average ± SD (n = 2–4 or 3–4/group, respectively). Data in tumor growth studies are average ± SE (n = 3–5/group).

RESULTS

Antiangiogenic Therapy

Bevacizumab therapy proved effective (Fig. 1) as at 10 mg/kg it halted tumor growth of both FaDu and SK-RC-52 tumor xenografts (Fig. 1). As early as 4 d after the start of therapy, growth of SK-RC-52 tumor xenografts was inhibited significantly, with tumor volumes equaling 15 ± 9 and 10 ± 3 mm^3 in control and treated mice, respectively ($P \leq 0.05$; Fig. 1A). The growth of FaDu tumor xenografts was halted significantly at 11 d after the start of therapy; tumor volumes were 362 ± 129 and 134 ± 121 mm^3 in control and treated mice, respectively (Fig. 1B). On the other hand, injection of 1 mg of bevacizumab per kilogram did not affect tumor growth in FaDu tumor xenografts (data not shown).

Tumor uptake of ^{111}In-RGD$_2$ after bevacizumab treatment did not differ significantly from controls (Fig. 2). At 2 d after the start of therapy, uptake of ^{111}In-RGD$_2$ within SK-RC-52 tumors was 4.78 ± 0.26 and 5.18 ± 0.49 %ID/g in control and treated mice, respectively (Fig. 2A). Figure 2B shows similar results for the FaDu tumors, with uptake of ^{111}In-RGD$_2$ equaling 1.28 ± 0.20 and 1.30 ± 0.54 %ID/g in control and treated mice, respectively, at day 3.

Nevertheless, uptake of ^{111}In-RGD$_2$, when expressed as %ID/tumor, did differ for FaDu xenografts (Figs. 2C and 2D). At 10 d after the start of bevacizumab therapy, tumor uptake of ^{111}In-RGD$_2$ was 0.30 ± 0.03 %ID and 0.16 ± 0.03 %ID, in control and treated mice, respectively ($P < 0.05$). Nonspecific uptake remained unaltered (Table 1).

Sorafenib therapy was not effective at 0.25 mg/mouse but did halt tumor growth at doses of 0.75 mg/mouse or greater as early as 5 d after the start of therapy (data not shown; Fig. 3A), with tumor volumes

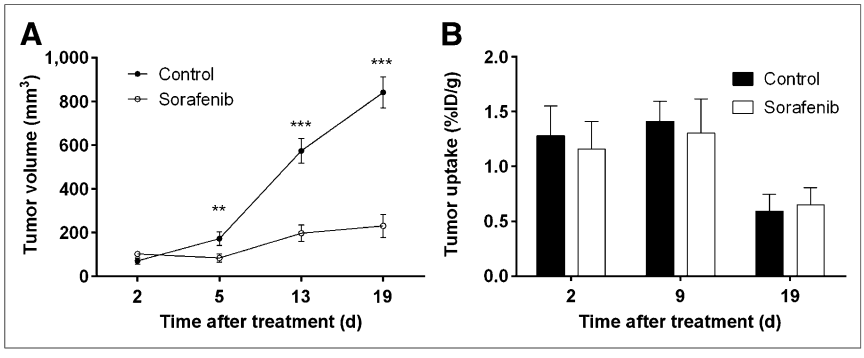

FIGURE 3. Sorafenib therapy. Tumor growth (A) and biodistribution (B) study in mice with FaDu xenografts treated with sorafenib. $^{**}P \leq 0.01$. $^{***}P \leq 0.001$.

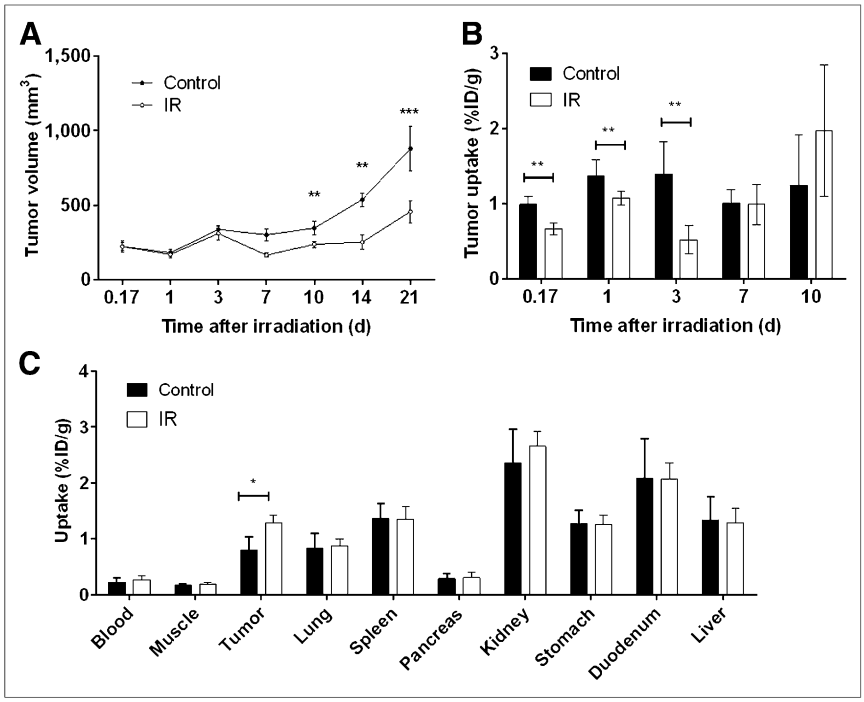

FIGURE 4. Radiation therapy. Tumor growth (A) and biodistribution (B) studies in irradiated (IR) mice with FaDu xenografts. (C) Tracer uptake in tissues at day 15 after local irradiation. $^{*}P \leq 0.05$. $^{**}P \leq 0.01$. $^{***}P \leq 0.001$.

equaling 172 ± 90 and 84 ± 55 mm^3 in control and treated mice, respectively.

The uptake of ^{111}In-RGD_2 in FaDu tumor xenografts does not differ between control and sorafenib-treated mice (Fig. 3B). At 9 d after the start of therapy, tumor uptake of ^{111}In-RGD_2 equaled 1.41 ± 0.18 and 1.30 ± 0.31 %ID/g for control and sorafenib groups, respectively.

Radiation Therapy

Local irradiation of FaDu tumors was effective in halting tumor growth. Ten days after irradiation, tumor volumes equaled 347 ± 124 and 238 ± 58 mm^3 in control and irradiated mice, respectively (Fig. 4A). At day 21 after irradiation, this effect was even more substantial; tumor volumes were 878 ± 414 and 457 ± 212 mm^3 in control and locally irradiated mice, respectively.

In irradiated FaDu tumors, the uptake of ^{111}In-RGD_2 altered significantly as early as 4 h (0.17 d) after local irradiation; uptake values were 0.99 ± 0.11 and 0.67 ± 0.08 %ID/g in control and locally irradiated mice, respectively ($P < 0.01$; Fig. 4B). At 7 d after irradiation, the significant decrease in tracer uptake within FaDu tumor xenografts was absent. At 15 d after irradiation, the opposite trend is observed as tumor uptake of ^{111}In-RGD_2 is significantly enhanced after local irradiation (1.28 ± 0.14 %ID/g), compared with nonirradiated mice (0.80 ± 0.23 %ID/g; Fig. 4C).

Non–Target-Mediated Effects

Tables 1 and 2 show that in general, bevacizumab or sorafenib treatment of mice bearing either SK-RC-52 or FaDu tumor xenografts did not affect nonspecific tumor uptake of ^{111}In-RGD_2 as determined by the coinjection of an excess of unlabeled RGD_2. For example, tumor uptake within SK-RC-52 tumors at 10 d after the start of bevacizumab therapy equaled 0.48 ± 0.05 and 0.48 ± 0.07 %ID/g in control and treated animals, respectively (Table 1). Also, nonspecific uptake of ^{111}In-RGD_2 in control and sorafenib-treated mice did not alter until day 19 after the start of therapy, with uptake values ratios equaling 0.19 ± 0.01 and 0.28 ± 0.03 in control and treated mice, respectively (Table 2). Table 3 shows that local tumor irradiation did not affect the uptake of ^{111}In-RGD_2 plus an excess of nonlabeled RGD_2, as tumor uptake values equaled 0.44 ± 0.06 and 0.59 ± 0.28 %ID/g in control and locally irradiated mice, respectively, at day 7 after irradiation.

Micro-SPECT/CT Imaging and Quantitative SPECT Analysis

In fused SPECT/CT scans, FaDu tumors were visualized with ^{111}In-labeled RGD_2. Tumor uptake of ^{111}In-RGD_2 mainly localized to the periphery of the tumor (Fig. 5).

Quantitative analysis of SPECT images showed that uptake of ^{111}In-RGD_2 (%ID/g) within the tumor decreased at 1 d after irradiation (0.30 ± 0.07 %ID/g), compared with nonirradiated controls (0.53 ± 0.45 %ID/g) ($P < 0.05$), yet was enhanced at day 15 in irradiated tumors (0.60 ± 0.18 %ID/g), compared with controls (0.22 ± 0.07 %ID/g) ($P = 0.06$; Fig. 6A). The uptake in the rim of tumors (0.51 ± 0.27 %ID/g), as measured by quantitative SPECT, was significantly enhanced in tumors of nonirradiated mice, compared with the uptake of ^{111}In-RGD_2 in the whole tumor ($P = 0.02$; Fig. 6A).

TABLE 2
Uptake (%ID/g) of ^{111}In-RGD_2 Plus 50 μg of RGD_2 in FaDu Xenografts in Mice Treated with Sorafenib

Time after treatment (d)	FaDu	
	Control	Sorafenib
2	0.44 ± 0.21	0.32 ± 0.09
9	0.40 ± 0.04	0.50 ± 0.12
19	0.19 ± 0.01	0.28 ± 0.03*

*$P \leq 0.05$.

TABLE 3
Uptake (%ID/g) of ^{111}In-RGD_2 Plus 50 μg of RGD_2 in Irradiated FaDu Xenografts

Time after treatment (d)	FaDu	
	Control	Irradiation
0.17	0.37 ± 0.04	0.33 ± 0.04
1	0.40 ± 0.14	0.38 ± 0.08
3	0.53 ± 0.20	0.50 ± 0.50
7	0.44 ± 0.06	0.59 ± 0.28
10	0.34 ± 0.05	0.51 ± 0.28

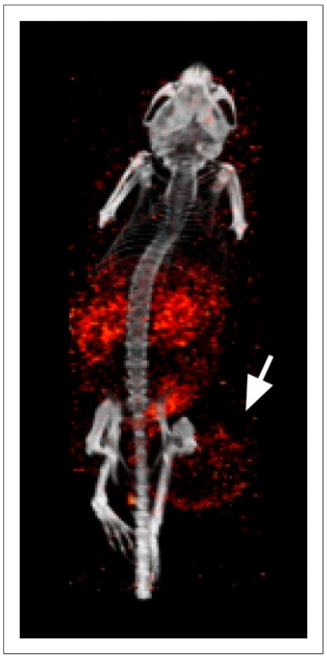

FIGURE 5. Representative 3-dimensional micro-SPECT/CT image of BALB/c *nu/nu* mouse with subcutaneous FaDu tumor xenograft on its right hind limb (arrow).

Correlation analysis of tumor uptake of ^{111}In-RGD$_2$, measured by quantitative SPECT, and tumor uptake of ^{111}In-RGD$_2$, measured in ex vivo biodistribution studies, confirmed that uptake can be monitored noninvasively by imaging, with a Spearman r value of 0.6 (Fig. 6B).

Immunohistochemistry

The immunohistochemical results for integrin β_3 expression on murine vasculature (CD61) in mice treated with antiangiogenic therapy or radiation therapy are summarized in Table 4. No significant changes in either integrin β_3 (Table 4) or 9F1 expression (data not shown) were observed at any time point.

DISCUSSION

Here, the potential of ^{111}In-RGD$_2$ to act as a tool to monitor the effect on angiogenesis of antiangiogenic or radiation therapy was investigated. The HNSCC xenografts used in these studies express only integrin $\alpha_v\beta_3$ on angiogenic blood vessels, making them an ideal model for studies involving RGD tracers and angiogenesis. Some studies also suggested that these tracers could monitor response to antiangiogenic therapy in integrin $\alpha_v\beta_3$–overexpressing tumor models, which corresponds with monitoring viable tumor mass (*16,19*); we therefore also studied integrin $\alpha_v\beta_3$–overexpressing tumors.

The results show that treatment of mice with bevacizumab, sorafenib, or radiotherapy was effective in inhibiting tumor growth (Figs. 1, 3A, and 4A). Interestingly, 29 d after the start of treatment with bevacizumab, growth of FaDu tumor xenografts recovered to the same rate as in nontreated mice, suggesting that the effect of bevacizumab had worn off.

^{111}In-RGD$_2$ proved a good tool to monitor changes, or as in this study the lack of changes, either in angiogenesis (FaDu) or in integrin $\alpha_v\beta_3$ expression on both vessels and tumor cells (SK-RC-52) after antiangiogenic treatment (Figs. 2 and 3B). As expected, uptake of ^{111}In-RGD$_2$ was higher in SK-RC-52 tumors than in FaDu tumors (Figs. 2A and 2B). Tracer uptake was unaltered after antiangiogenic therapy, even when tumor growth inhibition was apparent. This lack of effect is not due to altered accessibility of the tracer to the tumor, as nonspecific tracer uptake did not change after therapy (Tables 1 and 2). It is therefore likely that these antiangiogenic therapies did not alter integrin β_3 (Table 4) expression, or even 9F1 expression, despite a clear antitumor effect. This notion fits with hypotheses in which integrin $\alpha_v\beta_3$ negatively regulates angiogenesis (*24*). Also, results may have been influenced by the fact that no mouse surrogate anti–vascular endothelial growth factor antibody was used and bevacizumab is known to alter integrin $\alpha_v\beta_5$, rather than integrin $\alpha_v\beta_3$ (*25*). This would not have affected tumor uptake of divalent RGD radiotracers, which have no affinity for other integrins such as $\alpha_v\beta_5$, $\alpha_5\beta_1$, or $\alpha_{IIb}\beta_3$, with a 50% inhibitory concentration of greater than 10 mM as described previously (*26*).

Interestingly, treatment with sorafenib affected nonspecific uptake of ^{111}In-RGD$_2$ only at day 19 (Table 2), which might be explained by the fact that sorafenib is a multikinase inhibitor—it inhibits tumor growth directly (early) and affects angiogenesis later. Figures 2C and 2D suggest that ^{111}In-RGD$_2$ is only able to monitor tumor growth after antiangiogenic therapy and it would therefore not give any more specific or earlier information than standard Response Evaluation Criteria in Solid Tumors currently used clinically.

Monitoring angiogenesis is also important when considering HNSCC patients, whose treatment can include surgery, radiotherapy, and chemotherapy, which often have a negative impact on patients' quality of life. Despite advances in treatment possibilities, more than 50% of patients will relapse because of treatment resistance. Being able to noninvasively monitor early on whether patients respond to therapy would allow clinicians to determine whether the treatment should be adjusted to improve patient outcome as well as quality of life.

In irradiation experiments, ^{111}In-RGD$_2$ proved a good, early, and sensitive tool to monitor changes in angiogenesis (Figs. 4–6). In biodistribution studies (Figs. 4B), it was shown that uptake of ^{111}In-RGD$_2$ in FaDu tumors decreased shortly after irradiation, whereas tumor growth was not yet significantly altered (Fig. 4A) and decreased integrin expression was not yet obvious through immunohistochemical stainings (Table 4).

Tumor uptake of ^{111}In-RGD$_2$ increased beyond that in controls at day 15, as seen in both biodistribution and quantitative micro-SPECT studies (Figs. 4C and 6A). Quantitative micro-SPECT, however, did not pick up the significantly decreased or enhanced uptake of the tracer within the tumor at 4 h and 15 d after irradiation, respectively (Figs. 4B and 4C), suggesting that although ^{111}In-RGD$_2$ can be used as an in vivo imaging tool, its readout might not always be large enough to determine whether an effect is truly negative.

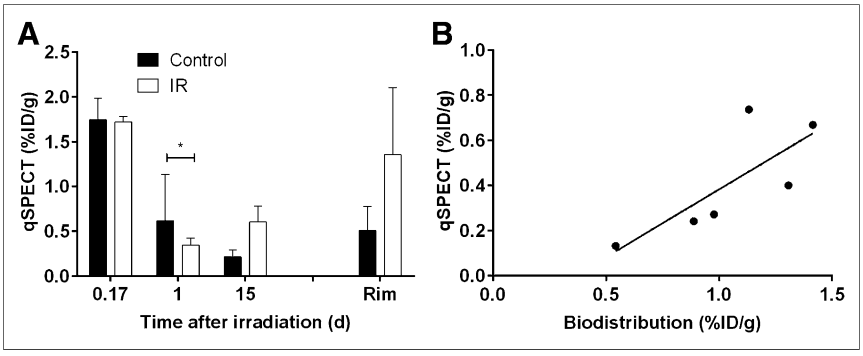

FIGURE 6. (A) Uptake of ^{111}In-RGD$_2$ within tumors or rim of tumors (day 15) as quantified from micro-SPECT images in irradiated (IR) mice (n = 2–3/group). (B) Tumor uptake of ^{111}In-RGD$_2$ at 15 d after tumor irradiation as quantified from micro-SPECT images plotted against values derived from biodistribution studies. *$P \leq 0.05$.

TABLE 4
Integrin β_3 Expression on New Blood Vessels (CD61) of FaDu Xenografts in Control Mice or Mice Treated with Bevacizumab, Sorafenib, or Local Irradiation

Time after treatment (d)	Control	Bevacizumab	Sorafenib	Irradiation
3	+	++		
10	+++	+++		
21	+++	++		
2	+		+	
5	++		++	
9	+++		+++	
19	++		+++	
0.17	++			++
1	++			++
3	++			++
10	++			+

+= ≤5%; ++ = 6%–10%; +++ = 11%–20%.

Nonspecific tracer uptake was not affected after irradiation (Table 3), suggesting that at time points up to 10 d after irradiation altered tumor uptake of ^{111}In-RGD$_2$ was due to a change in angiogenesis and not due to general tumor physiologic changes, such as perfusion or vascular permeability. Preliminary data using tumor sections stained for 9F1 (vascularity) and also imaged for Hoechst 33342 (perfusion), which was injected just 60 s before euthanasia, suggest that neither tumor vasculature nor perfusion was diminished in the early days after irradiation (data not shown). The sensitivity of the tracer is highlighted in Table 4, where immunohistochemical analysis of integrin β_3 expression remained unaltered after irradiation. Few studies have investigated the expression of integrin $\alpha_v\beta_3$ after irradiation of tumors; one study also showed that at 3 d after the last radiation fraction, expression of integrin $\alpha_v\beta_3$ in tumor xenografts was decreased (*27*). In vitro studies have also previously shown that integrin expression levels on endothelial cells can change within hours after radiotherapy (*28,29*).

Preliminary data suggest that perfusion is enhanced at day 15 in irradiated tumors by up to 40% when compared with nonirradiated tumors, which explains the enhanced tracer uptake at day 15. This finding could have major implications when planning the treatment schedules of patients for whom both radiotherapy and chemotherapy are used. On the other hand, an increased uptake of ^{111}In-RGD$_2$ at day 15 after irradiation could also be explained by an enhanced, though delayed, expression of integrin $\alpha_v\beta_3$, as suggested by other in vivo experiments (*27,30,31*). Nonetheless, the early and late effects of radiation on tumor vascularity, perfusion, and integrin $\alpha_v\beta_3$ expression require further investigation.

CONCLUSION

Here, it is suggested that ^{111}In-RGD$_2$ could allow in vivo monitoring of angiogenic responses after radiotherapy, but not antiangiogenic therapy, in HNSCC mouse models, indicating that, despite clear antitumor activity, antiangiogenic therapy in these tumor models does not have a mode of action driven by or affecting integrin $\alpha_v\beta_3$ expression. ^{111}In-RGD$_2$ may monitor both noninvasively and early on whether HNSCC patients respond to radiation therapy.

DISCLOSURE

The costs of publication of this article were defrayed in part by the payment of page charges. Therefore, and solely to indicate this fact, this article is hereby marked "advertisement" in accordance with 18 USC section 1734. Samantha Terry was funded by the Roche Postdoc Fellowship (RPF) Program. No other potential conflict of interest relevant to this article was reported.

ACKNOWLEDGMENTS

We thank Bianca Lemmers-van de Weem, Iris Lamers-Elemans, Kitty Lemmens-Hermans, and Henk Arnts for biotechnical assistance.

REFERENCES

1. Weis SM, Cheresh DA. Tumor angiogenesis: molecular pathways and therapeutic targets. *Nat Med.* 2011;17:1359–1370.
2. Hanahan D, Weinberg RA. Hallmarks of cancer: the next generation. *Cell.* 2011;144:646–674.
3. Gaertner FC, Schwaiger M, Beer AJ. Molecular imaging of $\alpha_v\beta_3$ expression in cancer patients. *Q J Nucl Med Mol Imaging.* 2010;54:309–326.
4. Zhu L, Niu G, Fang X, Chen X. Preclinical molecular imaging of tumor angiogenesis. *Q J Nucl Med Mol Imaging.* 2010;54:291–308.
5. Terry SY, Rijpkema M, Abiraj K, van der Graaf WT, Oyen WJ, Boerman OC. Radiolabeled imaging probes targeting angiogenesis for personalized medicine. *Curr Pharm Des.* 2014;20:2293–2307.
6. Dijkgraaf I, Kruijtzer JA, Frielink C, et al. $\alpha_v\beta_3$ integrin-targeting of intraperitoneally tumors with a radiolabeled RGD peptide. *Int J Cancer.* 2007;120:605–610.
7. Dijkgraaf I, Liu S, Kruijtzer JA, et al. Effects of linker variation on the in vitro and in vivo characteristics of an ^{111}In-labeled RGD peptide. *Nucl Med Biol.* 2007;34:29–35.
8. Dijkgraaf I, Terry SY, McBride WJ, et al. Imaging integrin $\alpha_v\beta_3$ expression in tumors with an ^{18}F-labeled dimeric RGD peptide. *Contrast Media Mol Imaging.* 2013;8:238–245.
9. Dijkgraaf I, Yim CB, Franssen GM, et al. PET imaging of $\alpha_v\beta_3$ integrin expression in tumours with ^{68}Ga-labelled mono-, di- and tetrameric RGD peptides. *Eur J Nucl Med Mol Imaging.* 2011;38:128–137.

10. Dumont RA, Deininger F, Haubner R, Maecke HR, Weber WA, Fani M. Novel ^{64}Cu- and ^{68}Ga-labeled RGD conjugates show improved PET imaging of $\alpha_v\beta_3$ integrin expression and facile radiosynthesis. *J Nucl Med.* 2011; 52:1276–1284.
11. Huang R, Vider J, Kovar JL, et al. Integrin $\alpha_v\beta_3$-targeted IRDye 800CW near-infrared imaging of glioblastoma. *Clin Cancer Res.* 2012;18:5731–5740.
12. Li ZB, Chen K, Chen X. ^{68}Ga-labeled multimeric RGD peptides for microPET imaging of integrin $\alpha_v\beta_3$ expression. *Eur J Nucl Med Mol Imaging.* 2008;35:1100–1108.
13. Oxboel J, Brandt-Larsen M, Schjoeth-Eskesen C, et al. Comparison of two new angiogenesis PET tracers ^{68}Ga-NODAGA-E[c(RGDyK)]$_2$ and ^{64}Cu-NODAGA-E[c(RGDyK)]$_2$; in vivo imaging studies in human xenograft tumors. *Nucl Med Biol.* 2014;41:259–267.
14. Terry SY, Abiraj K, Frielink C, et al. Imaging integrin $\alpha_v\beta_3$ on blood vessels with ^{111}In-RGD$_2$ in head and neck tumor xenografts. *J Nucl Med.* 2014;55:281–286.
15. Haubner R, Wester HJ, Weber WA, et al. Noninvasive imaging of $\alpha_v\beta_3$ integrin expression using ^{18}F-labeled RGD-containing glycopeptide and positron emission tomography. *Cancer Res.* 2001;61:1781–1785.
16. Battle MR, Goggi JL, Allen L, Barnett J, Morrison MS. Monitoring tumor response to antiangiogenic sunitinib therapy with ^{18}F-fluciclatide, an ^{18}F-labeled $\alpha_v\beta_3$ integrin and $\alpha_v\beta_5$ integrin imaging agent. *J Nucl Med.* 2011;52:424–430.
17. Dumont RA, Hildebrandt I, Su H, et al. Noninvasive imaging of $\alpha_v\beta_3$ function as a predictor of the antimigratory and antiproliferative effects of dasatinib. *Cancer Res.* 2009;69:3173–3179.
18. Goggi JL, Bejot R, Moonshi SS, Bhakoo KK. Stratification of ^{18}F-labeled PET imaging agents for the assessment of antiangiogenic therapy responses in tumors. *J Nucl Med.* 2013;54:1630–1636.
19. Ji S, Zheng Y, Shao G, Zhou Y, Liu S. Integrin $\alpha_v\beta_3$-targeted radiotracer ^{99m}Tc-3P-RGD$_2$ useful for noninvasive monitoring of breast tumor response to antiangiogenic linifanib therapy but not anti-integrin $\alpha_v\beta_3$ RGD$_2$ therapy. *Theranostics.* 2013;3:816–830.
20. Samant RS, Shevde LA. Recent advances in anti-angiogenic therapy of cancer. *Oncotarget.* 2011;2:122–134.
21. Hoogsteen IJ, Marres HA, van der Kogel AJ, Kaanders JH. The hypoxic tumour microenvironment, patient selection and hypoxia-modifying treatments. *Clin Oncol (R Coll Radiol).* 2007;19:385–396.
22. Wechsel HW, Petri E, Feil G, Nelde HJ, Bichler KH, Loesr W. Renal cell carcinoma: immunohistological investigation of expression of the integrin $\alpha_v\beta_3$. *Anticancer Res.* 1999;19:1529–1532.
23. van der Have F, Vastenhouw B, Ramakers RM, et al. U-SPECT-II: an ultra-high-resolution device for molecular small-animal imaging. *J Nucl Med.* 2009; 50:599–605.
24. Hynes RO. A reevaluation of integrins as regulators of angiogenesis. *Nat Med.* 2002;8:918–921.
25. Friedlander M, Brooks PC, Shaffer RW, Kincaid CM, Varner JA, Cheresh DA. Definition of two angiogenic pathways by distinct α_v integrins. *Science.* 1995;270:1500–1502.
26. Harris TD, Cheesman E, Harris AR, et al. Radiolabeled divalent peptidomimetic vitronectin receptor antagonists as potential tumor radiotherapeutic and imaging agents. *Bioconjugate Chem.* 2007;18:1266–1279.
27. Ning S, Nemeth JA, Hanson RL, Forsythe K, Knox SJ. Anti-integrin monoclonal antibody CNTO 95 enhances the therapeutic efficacy of fractionated radiation therapy in vivo. *Mol Cancer Ther.* 2008;7:1569–1578.
28. Albert JM, Cao C, Geng L, Leavitt L, Hallahan DE, Lu B. Integrin $\alpha_v\beta_3$ antagonist Cilengitide enhances efficacy of radiotherapy in endothelial cell and non-small-cell lung cancer models. *Int J Radiat Oncol Biol Phys.* 2006;65:1536–1543.
29. Abdollahi A, Griggs DW, Zieher H, et al. Inhibition of $\alpha_v\beta_3$ integrin survival signaling enhances antiangiogenic and antitumor effects of radiotherapy. *Clin Cancer Res.* 2005;11:6270–6279.
30. Ning S, Tian J, Marshall DJ, Knox SJ. Anti-α_v integrin monoclonal antibody intetumumab enhances the efficacy of radiation therapy and reduces metastasis of human cancer xenografts in nude rats. *Cancer Res.* 2010;70:7591–7599.
31. Mikkelsen T, Brodie C, Finniss S, et al. Radiation sensitization of glioblastoma by cilengitide has unanticipated schedule-dependency. *Int J Cancer.* 2009; 124:2719–2727.